

Limits of Blue and Green Infrastructures to Adapt Actual Urban Drainage Systems to the Impact of Climate Change

Thomas Benoit¹; Jean-Luc Martel, Ph.D.²; Émilie Bilodeau³; François Brissette, Ph.D.⁴; Alain Charron⁵; Dominic Brulé⁶; Gilles Rivard⁷; and Simon Deslauriers⁸

Abstract: Urbanization over the last few decades has resulted in a rise of impervious surfaces in municipalities worldwide. This rise has led to an increase in stormwater runoff and a decrease in the capacity of existing urban drainage systems. Additionally, the projected increase in frequency and intensity of extreme rainfall events due to climate change further exacerbates the risk of urban flooding. In response to this challenge, many municipalities have begun implementing blue and green infrastructures (BGI) to mimic the natural hydrologic cycle and manage stormwater at its source. Although the benefits of BGI, such as bioretention cells, permeable pavement, blue roofs, and green roofs, have been demonstrated, their full potential remains uncertain. This raises the question of whether BGI, when utilized to the maximum potential, can effectively adapt our existing drainage infrastructures to the projected increases in extreme rainfall in a warmer climate. To address this question, a case study was conducted in the Pointes-aux-Trembles District, a 20-km² urban catchment in Montreal. A calibrated stormwater management model [personnel computer storm water management model (PCSWMM)] was used to simulate various scenarios of BGI implementation, both individually and in combination without considering economic constraints. An extreme rainfall event was simulated under a warming climate to compare urban flooding between the existing urban drainage system and the different BGI scenarios. The results demonstrated the significant potential of BGI in adapting our existing drainage systems to climate change. In the simulated scenario of climate change impact, which resulted in a 136% increase in flood volume, the individual implementation scenarios offset between 20% and 118% of this increase. Furthermore, the combination scenarios achieved offsets of 162% and 167%, resulting in a better performance of the urban drainage systems (UDS) under climate change conditions with BGI practices than in historical conditions without any BGI practice. These findings strongly suggest that BGI practices should be considered as a crucial part of the adaptation solution. **DOI: 10.1061/JIJDH.IRENG-10330.** This work is made available under the terms of the Creative Commons Attribution 4.0 International license, <https://creativecommons.org/licenses/by/4.0/>.

Practical Applications: The growing trend of urbanization leads to an increase in impervious surfaces across municipalities worldwide, which in turn exacerbates stormwater runoff managed by urban drainage systems. Compounded by climate change, this trend heightens flood risks. To counteract this, many municipalities are adopting BGI, which mimic the natural hydrological cycle, to manage stormwater at its source. Although BIGs are recognized for their benefits, their full potential is yet to be fully understood. This case study utilized a stormwater management model in a district of Montreal to simulate various BGI implementation scenarios without considering economic constraints. The results indicated significant potential for BGIs to adapt UDS to the impact of climate change. When implemented, individual types of BGIs showed potential to offset between 20% to 118% of the increase in flood volume. Scenarios that combined different BGIs showed even more promise, reducing flooding by 162% to 167%. These outcomes not only mitigate the impact of climate change but also enhance the current capacity of UDS. In conclusion, BGIs represent a promising solution to the dual challenges of urbanization and climate change by effectively managing stormwater and enhancing the resilience of municipalities to flooding.

¹Master's Student, Hydrology, Climate, and Climate Change Laboratory, École de Technologie Supérieure, 1100 Notre-Dame St. West, Montreal, QC, Canada H3C 1K3. ORCID: <https://orcid.org/0009-0002-9771-5864>. Email: thomas.benoit.1@ens.etsmtl.ca

²Professor, Hydrology, Climate, and Climate Change Laboratory, École de Technologie Supérieure, 1100 Notre-Dame St. West, Montreal, QC, Canada H3C 1K3 (corresponding author). ORCID: <https://orcid.org/0000-0001-7142-6875>. Email: jean-luc.martel@etsmtl.ca

³Ph.D. Candidate, Hydrology, Climate, and Climate Change Laboratory, École de Technologie Supérieure, 1100 Notre-Dame St. West, Montreal, QC,

Canada H3C 1K3. ORCID: <https://orcid.org/0009-0005-8768-3637>. Email: emilie.bilodeau.1@ens.etsmtl.ca

⁴Professor, Hydrology, Climate, and Climate Change Laboratory, École de Technologie Supérieure, 1100 Notre-Dame St. West, Montreal, QC, Canada H3C 1K3. Email: francois.brissette@etsmtl.ca

⁵Director—Urban Hydrology, Lasalle Northwest Hydraulic Consultants, 9620 Saint-Patrick St., Montreal, QC, Canada H8R 1R8. Email: acharron@lasallenhc.com

⁶Engineer, Water Service, City of Montreal, 12001 Maurice-Duplessis Blvd., Montréal, QC, Canada H1C 1V3. Email: dominic.brule@montreal.ca

⁷Vice President—Urban Hydrology, Lasalle Northwest Hydraulic Consultants, 9620 Saint-Patrick St., Montreal, QC, Canada H8R 1R8. Email: grivard@lasallenhc.com

⁸Project Engineer, Lasalle Northwest Hydraulic Consultants, 9620 Saint-Patrick St., Montreal, QC, Canada H8R 1R8. Email: sdeslauriers@lasallenhc.com

Note. This manuscript was submitted on November 20, 2023; approved on September 9, 2024; published online on January 11, 2025. Discussion period open until June 11, 2025; separate discussions must be submitted for individual papers. This paper is part of the *Journal of Irrigation and Drainage Engineering*, © ASCE, ISSN 0733-9437.

Introduction

Over the last few decades, urbanization has led to increased impermeable surfaces and loss of permeable soil surfaces, disrupting the natural hydrological cycle by impeding water infiltration into the ground. This has resulted in an increase in both the volume and peak flow of runoff during rainfall events (Leopold 1968; Lee and Heaney 2003; Akter et al. 2018). Traditional urban drainage systems (UDS), consisting of gutters, pipes, and tunnels, were constructed to rapidly remove local runoff from urban areas and discharge it into nearby streams (Sohn et al. 2019; Tansar et al. 2022). However, these systems were designed without considering the ongoing changes in land use, which led to a significant increase in impervious surfaces in urban areas. Consequently, many UDS in municipalities worldwide are now outdated, making them inadequate for effectively handling runoff during extreme rainfall events, which increases the vulnerability of these municipalities to pluvial flooding (Pour et al. 2020; Yang et al. 2020).

Furthermore, drainage infrastructures were built based on statistical analysis of past rainfall events, assuming that the climate would remain stationary throughout their life span (Arisz and Burrell 2006). However, it is now widely accepted that climate change is already causing, and will continue to cause, more intense and frequent extreme rainfall events (Martel et al. 2020; IPCC 2021; Fowler et al. 2021). As a consequence, the limitations of existing UDS will be exacerbated, resulting in a higher probability of urban pluvial flooding events (Mailhot and Duchesne 2010; Mamo 2015; Martel et al. 2021).

Given the need to adapt existing UDS, municipalities should explore alternative strategies beyond traditional approaches. Upgrading the drainage capacity of these systems in developed areas is often considered expensive, impractical, and unsustainable due to ongoing urban development and the projected increase in rainfall intensity associated with climate change (Qin et al. 2013; Dong et al. 2017). As a climate change adaptation solution, there has been increasing interest in blue and green infrastructures (BGI) over the last two decades. BGI refers to a range of decentralized elements aimed at mitigating the adverse impacts of urbanization and climate change, particularly in stormwater management (Liu et al. 2019; Almaaitah et al. 2021).

BGI encompasses both green (GI) and blue infrastructures (BI). GI involves practices that mimic the natural hydrological cycle using vegetation and soil to manage rainfall through processes such as infiltration, evapotranspiration, retention, and detention. On the other hand, BI comprises nonvegetated practices that slow down runoff by providing temporary storage of rainfall, thereby mitigating peak discharge (Fletcher et al. 2015; Versini et al. 2018; USEPA 2019; Almaaitah et al. 2021). BGI also provides various cobenefits, including mitigating the urban heat island effect, improving livability, recharging groundwater, and supporting biodiversity (Liu et al. 2019).

As the recognition of BGI practices grows as potential adaptation solutions to the challenges faced by UDS, several studies have used hydrological models to simulate their implementation and assess their performance in supporting existing UDS:

- Zahmatkesh et al. (2015) evaluated the effectiveness of implementing rainwater harvesting practices, bioretention cells, and permeable pavement under various climate change scenarios. Through analysis of aerial images, land use, topography, and expert's judgment, they found that the combined implementation of these practices resulted in an average reduction of 41% in annual runoff volume in 30-year continuous simulations across different climate change scenarios. Additionally, they observed average annual maximum flow reductions ranging from

8% to 13%. In single-event simulations, they achieved runoff volume reductions of 28% and 14% for rainfall events with 2-year and 50-year return periods, respectively.

- Ahlblade and Shakya (2016) assessed the potential of permeable pavement, rain gardens, and rain barrels, individually and in combination, to mitigate flood risk in urban areas. The implementation rates of BGI practices varied from 25% to 100% of the available surface area for each BGI type. Their study demonstrated reductions ranging from 3% to 47% in average annual runoff and 0% to 40% in the number of flood events during 25-year continuous simulations based on historical rainfall data.
- Ghodsi et al. (2020) aimed to determine the optimal implementation of a combination of bioretention cells, vegetative swales, infiltration trenches, and permeable pavement to minimize runoff volume and BGI implementation cost under various climate change projections for both 2-year and 20-year return period design rainfall events. Their findings showed a runoff volume reduction of approximately 14% for BGI implementation on less than 1% of the catchment surface, highlighting the effectiveness of BGI practices even with a relatively small implementation area.
- Samouei and Özger (2020) investigated the impact of large-scale implementation of BGI practices on the hydrological response of an urbanized catchment. Their study revealed reductions in peak runoff ranging from 2.7% to 24.7% and runoff volume from 2.9% to 17% for a combined implementation of green roofs, permeable pavement, and bioretention cells. The implementation ratios ranged from 5% to 20% of the total catchment area.

Although BGI practices are receiving increasing attention in the literature and operational fields (Suleiman 2021), there is still a knowledge gap regarding their maximum potential to adapt actual UDS to the impacts of climate change. One key question that remains uncertain is whether these practices can offset the impact of climate change on the response of actual UDS to a future extreme rainfall event. Therefore, this study utilizes a previously developed high-resolution and calibrated personnel computer storm water management model (PCSWMM) model of a 20-km² urban catchment located in Montreal, Canada. The aim is to evaluate the maximum potential of a large-scale implementation, without economic constraints, of various BGI practices to counteract the projected impact of climate change on the response of the actual UDS under an extreme design storm event.

Methods

Study Area

This study focuses on the Pointe-aux-Trembles sector, which is a 20-km² urban catchment located in the easternmost borough of the City of Montreal, Canada. Montreal, the most populous city in the Province of Quebec, has a population of 2 million residents residing on the 500-km² island (Statistics Canada 2023). Since the mid-twentieth century, the city has undergone rapid urban development, resulting in a significant increase in urban sprawl since 1951. The Rivière-des-Prairies-Pointe-aux-Trembles borough, which includes the Pointe-aux-Trembles sector, has also experienced rapid urbanization in recent years, with urban sprawl tripling between 1986 and 2011 (Nazamia et al. 2016). Consequently, the Pointe-aux-Trembles sector is now highly urbanized, with residential areas dominating the land use.

The study area, as shown in Fig. 1, consists of 20 catchments that can be gathered in four independent subareas. The networks are predominantly composed of circular pipes with diameters

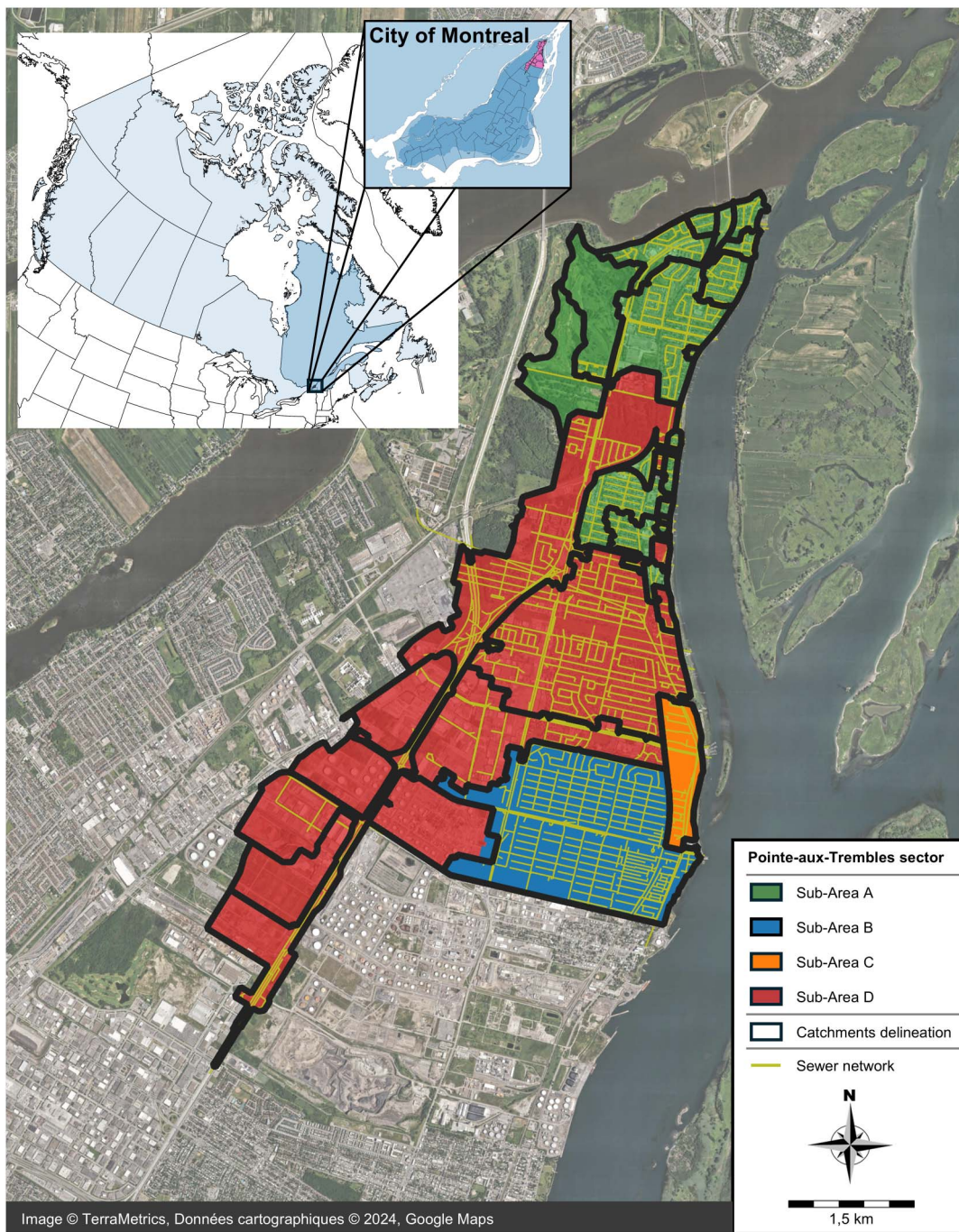


Fig. 1. View of the study area. The 20 catchments are delineated by bold lines. (Base map image © TerraMetrics, Données cartographiques © 2024, Google Maps.)

ranging from 150 mm to 3 m, with slopes ranging from 0.01% to 33.78%. It encompasses both combined and separated sewer systems. The combined systems transport both wastewater and stormwater via the southeast interceptor, which ranges in dimension from 3 to 5 m, either to the wastewater treatment plant or to the St. Lawrence River during events that cause combined sewer overflows (CSOs). During three rainfall events in 2011 and 2012, localized urban flooding issues were reported in the sector. A recurrence analysis of these rainfall events, based on a comparison with local intensity-duration-frequency (IDF) curves, revealed that their return periods ranged from 2 to 100 years, highlighting the vulnerability of the existing UDS to even relatively frequent extreme storm events.

PCSWMM Model of the Study Area

In 2018, the City of Montreal enlisted the services of Lasalle Northwest Hydraulic Consultants (NHC) to enhance an existing USEPA Storm Water Management Model version 5 (SWMM5) model of the Pointe-aux-Trembles District as part of its long-term planning for wastewater and stormwater management over the next 25 years. The objective was to utilize the model for a precise analysis of the current UDS performance in the area. PCSWMM combines the SWMM5 engine with an improved graphical user interface and additional tools to conduct analyses and GIS capabilities, serving as a spatial decision support tool for urban stormwater management (CHI 2023).

The SWMM5 engine is a dynamic rainfall-runoff simulation model that enables both single-event and long-term simulations to evaluate the quantity and quality of runoff, primarily in urban areas. It focuses on subcatchment areas that receive precipitation, generating runoff and pollutants loads. The routing aspect of SWMM5 involves the transportation of this runoff through a network consisting of pipes, channels, storage/treatment devices, pumps, and regulators. Throughout the simulation period, which includes multiple time steps, SWMM5 tracks the quantity and quality of runoff within each subcatchment, as well as the flow rate, flow depth, and water quality within the pipes and channels. SWMM5 is widely used worldwide to support planning, analysis, and design associated with stormwater runoff, combined sewers, sanitary sewers, and other drainage systems in urban areas (Rossman 2015).

The PCSWMM model of the study area incorporates an improved delineation of subcatchments, which distinguishes drained surfaces based on their physical characteristics and hydrological responses. This division categorizes the model into three types of subcatchments: road elements, flat roofs, and a broader category encompassing other land uses. This distinction enables an accurate representation of the rapid hydrological response of road elements and the potential retention capacity of flat roofs during intense rainfall events.

Road elements are individually modeled as subcatchments with an average area of 1,084 m². They have a high impermeability percentage of 90% and a flow length adjusted to accurately reflect the specific shape and hydrological response of a road. Each flat roof is modeled as a storage node, and its outflow is regulated by an outlet which is parameterized to simulate the behavior of an orifice. The number and diameter of roof drains are estimated on local building code. The remaining subcatchments represent various land uses in the study area, including commercial, industrial, residential, and recreational areas. The impervious percentage of these subcatchments is determined based on land-use occupation, ensuring an appropriate representation. They have longer flow lengths, and in some cases, a portion of their impervious area directs runoff toward their pervious area. Fig. 2 presents a detailed view of a part of the PCSWMM model, showing the three types of subcatchments.

The slope of each subcatchment has been set at 1% to account for the mostly flat topography of the study area, where slopes range from 0% to 1%. Additionally, the major network, constituted by the streets that move excess runoff when the capacity of catch basins is exceeded, was not modeled because the site's topography is relatively flat and there are enough catch basins to fully intercept runoff. It was determined that the surface network could effectively intercept runoff from a 3-h storm event with a 25-year return period across all 20 study areas' catchments. This was considered adequate for the original purpose of the model because the assessment of the existing UDS's service level was based on a design storm event with a 10-year return period.

To maintain a high spatial resolution while reducing computational time, the PCSWMM model was divided into four submodels that correspond to the four independent subareas of the study area. The study area, spanning 2.006 km², is divided into four submodels ranging from 0.052 to 1.091 km², encompassing a total of 9,935 subcatchments, 5,809 nodes, 5,951 conduits, 65 outfalls, and 17 hydraulic structures including pumping station, regulation, overflow, and diversion structures. Table 1 provides the characteristics of the four subareas, including the total impervious area and the surface areas occupied by each of the three subcatchment types.

Calibration of the PCSWMM Model

Calibration and validation of the model were conducted by comparing computed results with data obtained of flow measurements by the city from 2016 to 2017 at a 5-min time interval. Data were collected from 11 measurement points that covered the entire study area network, including four temporary and three permanent rain gauges.

The minimum, maximum, and mean flow rates during dry periods, along with data pertaining to population, surface area, and land use upstream of each measurement point, were utilized to compute consumption and infiltration indices. These indices were subsequently employed to allocate sanitary flows within the model, with each sanitary flow inlet node combining infiltration flow and ICI consumption into a fixed base flow; meanwhile, average residential consumption was linked to a time-based pattern according to population size.

For each measurement point, four rainfall events were used for calibration, and three additional events were used for validation. The seven events selected were the ones with the largest rainfall volumes recorded at the nearest rain gauge.

During the calibration process, adjustments were made primarily to the imperviousness of subcatchments in combined sewer system areas, and parameters of the unit hydrographs were fine-tuned in separated sewer system areas. The Nash-Sutcliffe efficiency (NSE) criterion was calculated to evaluate the model's ability to accurately replicate peak flow and volume at each measurement point. Comparing the computed and measured peak flows and volumes for the four calibration rainfall events, median NSE values of 0.88, 0.86, 0.67, and 0.82 were obtained for Subareas A, B, C, and D, respectively. For the three validation rainfall events, the median NSE values were 0.91, 0.88, 0.44, and 0.70 in Subareas A, B, C, and D, respectively. According to the literature, NSE values above 0.50 indicate a fair calibration (Moriasi et al. 2007; Shamsi and Koran 2017). Therefore, it was concluded that the models accurately represent the volumes and peak flows in the network of the study area.

The calibrated models were further used to validate the frequency and duration of overflow events at each overflow structure in the network. The majority of these structures were monitored by the city from 2014 to 2017. The analysis demonstrated that the models accurately reproduced a significant portion of the recorded overflow events during this period, with 80% of the city-recorded overflows being replicated in the model.

BGI Selection

Among the various BGI practices available for stormwater management, bioretention cells, permeable pavement, green roofs, and blue roofs are considered to be among the most common and effective techniques (Shafique et al. 2016; Samouei and Özger 2020). These practices can be adapted to different urban contexts, and studies have demonstrated their effectiveness in addressing water quantity and quality issues, even in cold climates (Drake et al. 2014; Johannessen et al. 2017; Ding et al. 2019). Thus, this study focused on evaluating the performance of these four options in mitigating the impact of climate change on the UDS study area.

Bioretention cells are depressions filled with a specially engineered soil mixture and vegetation. They provide temporary storage, infiltration, and evaporation of rainfall and runoff from adjacent areas (Rossman 2016). In urban areas, bioretention cells are commonly incorporated into curb extensions, sidewalks, or median reservations (STEP 2022).

Permeable pavements differs from a conventional impervious pavement because they allow water to drain through the surface



Fig. 2. Detailed view of a part of the PCSWMM model. (Base map image © 2024, Google Earth.)

Table 1. Characteristics of the four subareas

Subarea	Area (ha)	Impervious area (ha)	Impervious area (%)	Flat roofs (ha)	Flat roofs (%)	Road elements (ha)	Road elements (%)	Others (ha)	Others (%)
A	535.22	127.12	24	18.11	3	64.55	12	452.56	85
B	327.5	153.99	47	22.54	7	64.66	20	240.30	73
C	51.89	20.72	40	5.88	11	8.14	16	37.87	73
D	1,091.27	458.54	42	68.98	6	148.45	14	873.84	80

Note: Flat roofs, road elements, and others are the three types of subcatchment, and they add up to 100% of the area of each subarea.

and into a storage layer of gravel, enabling infiltration into the native soil or temporary detention (Rossman 2016). Permeable pavement systems are commonly used in parking lots, low-traffic roads, driveways, and pedestrian areas. This technology can also be

implemented in locations subject to heavier loads, such as commercial and industrial loading and storage areas (Imran et al. 2013; STEP 2022). The design of both bioretention cells and permeable pavement depends on factors like the infiltration potential of the

Table 2. Parameterization of the four BGI practices evaluated in this study

BGI layer	Parameter name (unit)	Bioretention cells	Permeable pavement	Green roofs	Blue roofs (rain barrel)
Surface	Berm/barrel height (mm)	150	0	0	50
	Vegetation volume (fraction)	0.05	0	0	—
	Surface roughness (Manning's n)	0	0.02	0.1	—
	Surface slope (%)	0	1	1	—
Pavement	Thickness (mm)	—	100	—	—
	Void ratio (voids/solids)	—	0.18	—	—
	Impervious surface (fraction)	—	0	—	—
	Permeability (mm/h)	—	2,540	—	—
	Clogging factor	—	0	—	—
Soil	Thickness (mm)	450	0	100	—
	Porosity (volume fraction)	0.43	—	0.5	—
	Field capacity (volume fraction)	0.13	—	0.2	—
	Wilting point (volume fraction)	0.08	—	0.1	—
	Conductivity (mm/h)	120	—	12.5	—
	Conductivity slope	35	—	35	—
	Suction head (mm)	50	—	50	—
Storage	Height (mm)	300	300	—	—
	Void ratio (voids/solids)	0.62	0.67	—	—
	Seepage rate (mm/h)	7.5 (or 0 ^a)	7.5 (or 0 ^a)	—	—
	Clogging factor	0	0	—	—
Drainage mat	Thickness (mm)	—	—	50	—
	Void fraction	—	—	0.3	—
	Roughness (Manning's n)	—	—	0.03	—
Underdrain	Drain coefficient (mm/h)	2.7	1.32	—	0.589
	Drain exponent	0.5	0.5	—	0.5
	Drain offset height (mm)	150 (or 0 ^a)	150 (or 0 ^a)	—	—
	Drain delay (h)	—	—	—	0

^aBGI modeled with an impermeable bottom liner.

native soil and site characteristics. They can be designed with no underdrain for complete infiltration, with an elevated underdrain for partial infiltration, or with an underdrain and impermeable bottom liner solely for detention and filtration purposes (STEP 2022).

Green roofs are a form of vegetated control designed for implementation on rooftops. They consist of a layer of vegetation grown in an engineered soil mixture, placed on a drainage mat that transports excess water from the soil layer outside of the roof (Rossman 2016). BGI practices on rooftops, such as green roofs, are widely adopted due to their significant potential, especially considering that roofs contribute a substantial portion of the impervious area in developed countries (Shafique et al. 2016). Among the different types of green roofs, extensive green roofs, which have a lower profile, have gained popularity in urban retrofitting projects and are commonly chosen (Hamouz and Muthanna 2019).

Blue roofs offer a cost-effective alternative to green roofs and are designed to temporarily detain stormwater on rooftops in non-vegetated ponding areas. Flow control devices at the inlets of the roof drains regulate the slow release of rainwater into the sewer or drainage network, effectively reducing peak flows. Blue roofs are particularly suitable for urban retrofitting projects focused on stormwater management in developed areas (Shafique et al. 2016).

Modeling BGI in PCSWMM

The SWMM5 engine has the capability to simulate the behavior of eight different types of BGI practices by incorporating them as properties of the subcatchments (Rossman 2015).

Bioretention cells, permeable pavement, and green roofs were modeled using their respective BGI practice modules in SWMM5.

The parameters for these BGIs were based on two studies conducted for the green infrastructure (GI) Leadership Exchange (GILE) initiative (Lotus 2018, 2021), which aimed to evaluate the possibility of creating North American standards for modeling bioretention cells, permeable pavement, infiltration trenches, and green roofs using the SWMM5 engine in terms of water quantity performance. The recommended modeling parameters provided by these studies were derived from a comprehensive review and analysis of existing modeling parameters from publicly available reports, internal documents, data from study collaborators, information available for regional and national stormwater calculators, peer-reviewed articles, and SWMM default parameters. Additionally, the national standard for the design of bioretention cells (CSA Group 2018) was considered when parameterizing bioretention cells.

Because blue roofs are not explicitly represented in the SWMM5 low impact development (LID) module (referred to as the BGI module hereafter for consistency), they were modeled using the rain barrel BGI practice to approximate a rooftop rainfall storage depth capacity of 50 mm, which is in line with local guidelines suggesting that large commercial roofs can store between 50 and 80 mm of rainwater (MDDEFP 2011). To simulate the gradual release of rainfall into the network, blue roofs were equipped with a drain parameterized to have a 24-h drawdown time when reaching full storage capacity. Modeling blue roofs using the rain barrel BGI practice does not consider the evaporation process typically occurring on blue roofs. This modeling approach is therefore conservative because it assumes that all rainfall falling on rooftops ultimately flows into the network.

Furthermore, an analysis of soil types, conducted using a GIS layer representing the surficial deposit mapping in the study area, revealed that certain areas were unsuitable for implementing BGI practices involving infiltration processes due to the presence of

Table 3. Scenarios simulated in this study

Scenario	Simulated impact of CC	BGI implemented	Impervious area occupied (%)				
			Study area	Subarea A	Subarea B	Subarea C	Subarea D
R_HC	No	None	—	—	—	—	—
R_CC	Yes	None	—	—	—	—	—
BIO	Yes	Bioretention cells	4	5	4	4	3
PP	Yes	Permeable pavement	14	8	10	9	17
GR	Yes	Green roofs	15	14	15	28	15
BR	Yes	Blue roofs	15	14	15	28	15
GIs	Yes	Bioretention cells, permeable pavement, green roofs	33	27	28	41	36
BGIs	Yes	Bioretention cells, permeable pavement, blue roofs	33	27	28	41	36

rock, mixed sediments, or peat. In these areas, bioretention cells and permeable pavement systems were parameterized to represent installations equipped with an impervious bottom liner and an underdrain, preventing any infiltration into the native soil. Conversely, in areas where the soil type allowed infiltration, bioretention cells and permeable pavement were modeled with an elevated underdrain to enable partial infiltration into the native soil. Table 2 presents the modeling parameters used in this study.

Design Storm Event

The model was supplied with input data for a design storm event based on IDF curves obtained from the meteorological station at Montreal International Airport. Specifically, a rainfall event lasting 3 h, with a return period of 10 years and following a Chicago-type temporal distribution, was selected to simulate the response of the actual UDS to an extreme storm event. The selected storm duration and return period align with the requirements set by the Quebec design code for flood control stormwater management structures (LégisQuébec 2022).

To incorporate the impact of climate change, the design storm event was subjected to a fixed increase of 18%. This increase in rainfall intensity reflects the minimal adjustment mandated by the Quebec Ministry of the Environment and Fight against Climate Change, Wildlife and Parks (MELCCFP) for storm events rarer than a 2-year return period (LégisQuébec 2022). This 18% fixed increase in rainfall intensity is referred to as the simulated impact of climate change (SICC) hereafter.

BGI Scenarios Simulated

A total of eight scenarios were simulated simultaneously in each of the four subareas of the Pointe-aux-Trembles study area network. To evaluate the impact of climate change on the response of the actual UDS to the design storm event, the first two scenarios were simulated without implementing any BGI practices:

1. R_HC: Response of the actual UDS to the design storm event under historical conditions.
2. R_CC: Response of the actual UDS to the design storm event considering the SICC.

Next, to evaluate the individual potential of the selected BGI practices in mitigating the impact of climate change on the response of the actual UDS to the design storm event, four scenarios simulated the large-scale implementation of a single BGI practice:

3. GR: Large-scale implementation of green roofs on every flat roof in the study area.
4. BR: Large-scale implementation of blue roofs on every flat roof in the study area.

5. PP: Large-scale implementation of permeable pavement in designated areas such as parking lots, industrial and commercial zones, school playgrounds, and sports courts. In industrial zones, the permeable pavement was parameterized to prevent infiltration into the native soil to avoid contamination from runoff loaded with pollutants (Yu et al. 2017).
6. BIO: Large-scale implementation of bioretention cells on every street in the study area. The runoff from these streets was directed entirely toward bioretention cells. The cells covered an average of 10% of the street surface, adhering to the recommended 1:10 ratio between the surface area of the cells and the surface area they drain (MDDEFP 2011; CSA Group 2018).

Finally, to evaluate the combined potential of these BGI practices, two remaining scenarios were simulated:

7. GIs: Large-scale implementation of green roofs, permeable pavement systems, and bioretention cells.
8. BGIs: Large-scale implementation of blue roofs, permeable pavement systems, and bioretention cells.

Table 3 summarizes the different scenarios modeled in this study and presents for each of them the percentage of impervious area occupied by the various BGI practices.

Metrics Evaluated

The evaluation of the SICC on the response of the actual UDS to the design storm event, as well as the potential of different BGI implementation scenarios to mitigate this impact, was based on the analysis of three metrics: runoff volume, outfall peak flow, and flood volume:

- Runoff volume: The total volume of water runoff generated in each subarea during the design storm event. This metric was used to assess variations in the hydrological response of the study area.
- Outfall peak flow: The maximum flow rate leaving the system at the outfall points in each subarea during the design storm event. This metric was used to evaluate variations in the hydraulic performance of the actual UDS.
- Flood volume: The total volume of water lost from model nodes in each subarea during the design storm event, i.e., water that could not be received by the network because the maximum conveyance capacity was reached. This metric was also used to assess variations in the hydraulic performance of the actual UDS.

To quantify the potential of each BGI implementation scenario in mitigating the SICC, the climate change offset (CCO) indicator was calculated. This indicator measures how closely each BGI scenario can achieve the historical climate condition value for each analyzed metric. The calculation of the CCO indicator is defined by Eq. (1)

$$CCO(S) = \frac{M_{R_CC} - M(S)}{M_{R_CC} - M_{R_HC}} \quad (1)$$

where $CCO(S)$ = percentage of the SICC that was offset by the BGI implementation scenario S on the metric M ; M_{R_CC} = value of the metric M under the R_CC scenario; M_{R_HC} = value of the metric M under the R_HC scenario; and $M(S)$ = value of the metric M under the BGI implementation scenario S . A similar method was used by Zahmatkesh et al. (2015) to evaluate the potential of a single BGI implementation scenario in offsetting different intensities of climate change impacts related to annual runoff volume.

By analyzing these metrics and the CCO indicator, the study aimed to provide a comprehensive assessment of the SICC on the UDS and the effectiveness of different BGI practices in offsetting the impact of climate change on the UDS's hydrological and hydraulic performance.

Results

Analysis of Runoff Volume

Fig. 3 presents the values of runoff volume for all eight simulated scenarios, as well as the values of the CCO indicator related to runoff volume for the six different BGI implementation scenarios in both the subareas [Figs. 3(a–d)] and the entire study area [Fig. 3(e)]. The runoff volume values for the overall study area are obtained by adding the corresponding values of the four subareas.

The results indicated that the SICC on the design storm event has a significant effect on increasing the runoff volume within the study area. Specifically, the SICC led to a 32% increase in the overall runoff volume [Fig. 3(e)], with similar percentages in Subareas B, C, and D [Figs. 3(b–d)]. Compared with the others, Subarea A exhibited a higher increase [Fig. 3(a)] due to its larger percentage of pervious area (Table 2), which becomes saturated and contributes to the increased runoff.

Upon evaluating the individual BGI implementation scenarios, it became apparent that none of them are capable of entirely offsetting the increase in runoff volume caused by the SICC. However, the scenario involving the implementation of bioretention cells (BIO) proved to be the most effective in mitigating the runoff volume. It offset approximately half of the SICC in both the overall study area and each subarea. The scenario involving green roofs (GR) ranked as the second most effective, surpassing the BIO scenario in Subarea C. This could be attributed to the higher contribution of flat roofs to the total impervious area in this specific subarea compared with the others (Table 3). In fact, both the GR and BR scenarios performed better in Subarea C compared with the other subareas. The scenario implementing blue roofs (BR) was least effective in reducing runoff volume because blue roofs only provide temporary detention of rainfall.

Upon analyzing the combined BGI implementation scenarios, it was evident that the GIs scenario, which combines green roofs, permeable pavement systems, and bioretention cells, came close to completely offsetting the increase in runoff volume caused by the SICC within the study area. It achieves a CCO value of 99%. In contrast, the BGIs scenario, which combines blue roofs, permeable

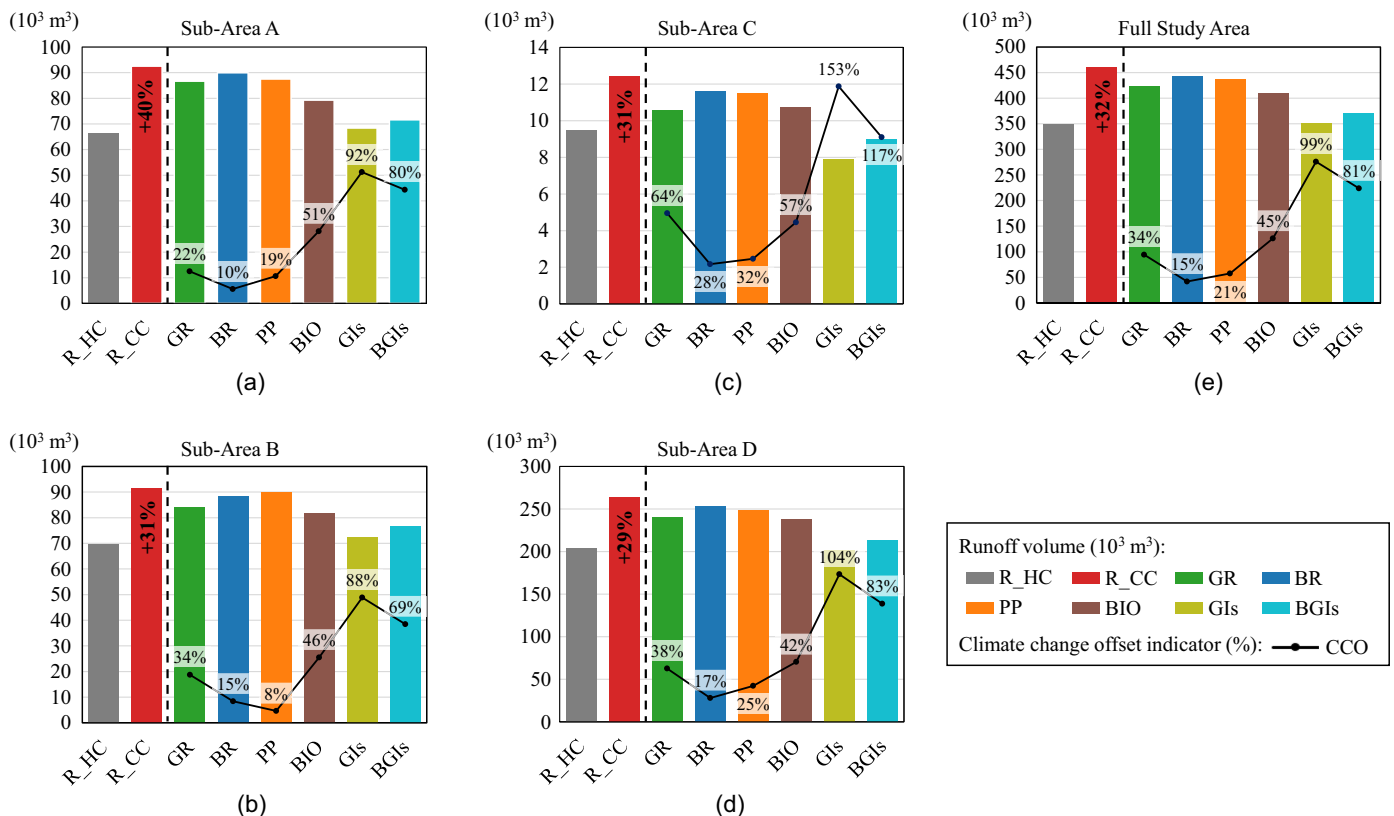


Fig. 3. Bar graphs of runoff volumes in all eight simulated scenarios (R_HC, R_CC, GR, BR, PP, BIO, GIs, and BGIs) and CCO indicator values (solid curve) for runoff volume in the six BGI implementation scenarios: (a) Subarea A; (b) Subarea B; (c) Subarea C; (d) Subarea D; and (e) the whole study area.

pavement systems, and bioretention cells, proved to be less effective than the GIs scenario in all subareas. This observation aligns with the fact that green roofs are more effective in reducing runoff volume compared with blue roofs. Notably, both the GIs and BGIs scenarios demonstrated the highest effectiveness in Subarea C, which can be attributed to the larger percentage of impervious area occupied by the combined BGI practices in this particular subarea.

Analysis of Outfall Peak Flow

In Fig. 4, the values of outfall peak flow for all eight simulated scenarios are presented for each subarea [Figs. 4(a–d)] as well as the entire study area [Fig. 4(e)]. Additionally, the values of the CCO indicator, with respect to the outfall peak flow, are provided for the six different scenarios BGI implementation. The outfall peak flow values for the overall study area are obtained by adding the corresponding values of the four subareas.

The results indicated that the impact of SICC on the design storm event led to a 20% overall increase in the response of the actual UDS in terms of outfall peak flow in the study area [Fig. 4(e)]. Specifically, Subareas A, B, C, and D [Figs. 4(a–d)] exhibited increases of 29%, 9%, 23%, and 20%, respectively. The relatively lower increase in Subarea B can be attributed to the fact that the R_HC scenario in this subarea had already reached its maximum network capacity. Consequently, the increase in peak flow at the outfalls was limited due to the restricted flow capacities. On the other hand, the higher increase in Subarea A can be attributed to the previously mentioned greater increase in runoff volume within this subarea.

Upon evaluating the individual BGI implementation scenarios, it became evident that the BIO scenario was the most effective in

mitigating the SICC on outfall peak flow. It completely offset the increase in each of the four subareas and even enhanced the performance of the UDS compared with its historical response. The higher CCO value in Subarea B can be attributed to a relatively lower increase in peak flow caused by the SICC compared with other subareas.

The PP scenario was the second most effective in mitigating outfall peak flow. It offset half of the increase in the entire study area. Subarea D exhibited the highest CCO value, which aligns with a higher implementation ratio of permeable pavement in this subarea compared with the others [Fig. 4(d)]. However, despite having a higher implementation ratio of permeable pavement than Subareas A and C, Subarea B showed a lower CCO value [Fig. 4(b)]. This can be partly attributed to a significant proportion of those permeable pavement systems in this subarea being parameterized with an unelevated underdrain, which makes them less effective in reducing peak flow.

Among the different BGI implementation scenarios, the GR scenario proved to be the least effective in mitigating outfall peak flow. The infiltration capacity of green roofs was exceeded by the intensity of rainfall, leading to overflow into the network and limited impact on peak flow reduction. On the other hand, the BR scenario demonstrated greater effectiveness in mitigating the SICC on outfall peak flow. It offset up to 84% of the SICC in Subarea C [Fig. 4(c)] due to the slow release of rainfall from blue roofs, which significantly reduced the peak flow from flat roofs.

When considering the combined BGI implementation scenarios, both the GIs and BGIs scenarios enhanced the performance of the UDS compared with its historical response. These scenarios entirely offset the SICC on outfall peak flow in every subarea. The higher performance of the BGIs scenario aligns with the superior

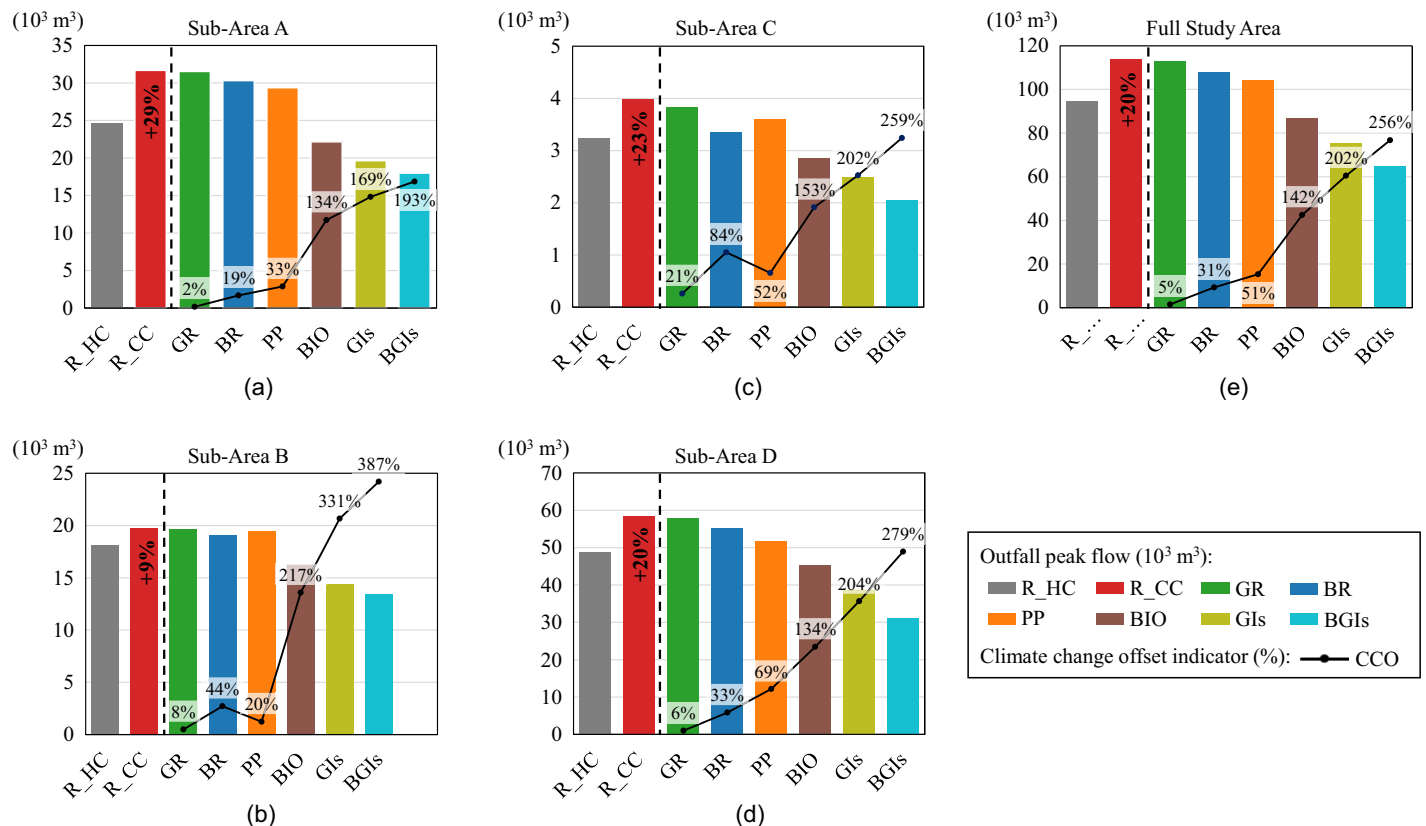


Fig. 4. Bar graphs of outfall peak flows for the eight simulated scenarios.

performance of the BR scenario compared with the GR scenario. Furthermore, the results also indicated that, except for the GR scenario, all the BGI implementation scenarios were more effective in mitigating the SICC on peak flow rather than on runoff volume for the design storm event.

Analysis of Flood Volume

In Fig. 5, the values of flood volume for all eight simulated scenarios are presented for each subarea [Figs. 5(a–d)] as well as the entire study area [Fig. 5(e)]. Additionally, the values of the CCO indicator, with respect to the flood volume, are provided for the six different scenarios of BGI implementation. The flood volume values for the study area are obtained by adding the corresponding values of the four subareas.

The analysis of the SICC on the response of the actual UDS regarding flood volume revealed a significant increase, with a global 136% rise in the study area [Fig. 5(e)]. The magnitude of the increases varied across the subareas, with Subarea C exhibiting the highest increase and Subarea D displaying the lowest increase. These results highlight the vulnerability of the actual UDS to the SICC because the increase in flood volume exceeded the increase in rainfall intensity by more than seven times.

When evaluating the individual BGI implementation scenarios, as expected based on previous results, the BIO scenario proved to be the most effective in mitigating the SICC on flood volume. It completely offset the increase in the study area and enhanced the performance of the UDS compared with its historical response. However, in Subarea A, the BIO scenario did not entirely offset the SICC on flood volume, despite having a higher implementation

ratio in this subarea compared with the others. This can be explained by the fact that the nodes contributing the most to flood volume in this subarea received significant volumes from large flat roofs, which are not impacted by bioretention cells.

Both the PP and BR scenarios offset more than two-thirds of the SICC on flood volume in the study area. The effectiveness of each scenario depends on the specific subarea, highlighting the influence of distinct catchment characteristics on the performance of BGI implementation. Notably, the GR scenario was less effective in mitigating the SICC on flood volume in Subarea C, despite a higher contribution of flat roofs to the total impervious area and a greater reduction in outfall peak flow compared with the other subareas. This can be attributed to the response of the UDS to the SICC regarding flood volume being more sensitive in Subarea C, and the peak flow reduction provided by green roofs being insufficient to prevent overflow at certain nodes.

Considering the combined BGI implementation scenarios, both the GIs and BGIs scenarios significantly enhanced the performance of the UDS compared with its historical response. They completely offset the SICC on flood volume in every subarea and effectively prevented the UDS from overflowing in Subareas C and D. The BGIs scenario showed only a slight advantage over the GIs scenario, except in Subarea A where the remaining flood volume was primarily influenced by nodes receiving significant volumes from large flat roofs. These nodes were less impacted by the peak flow reduction provided by green roofs. However, in other subareas, the combined effect of the BIO and PP scenarios freed up enough network capacity to prevent most nodes from overflowing, despite the relatively weaker performance of green roofs in reducing peak flow.

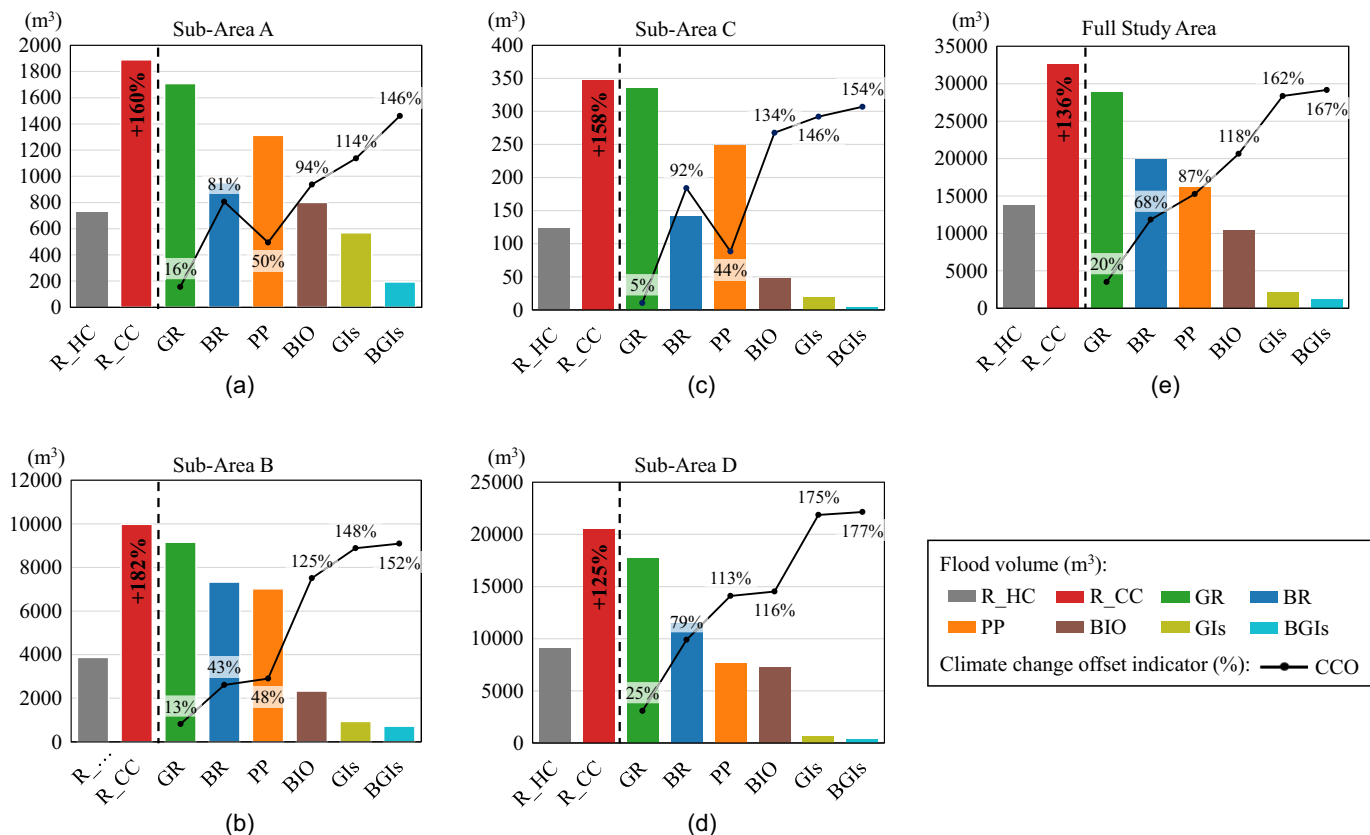


Fig. 5. Bar graphs of flood volume for the eight simulated scenarios.

Discussion

Potential of BGI to Counteract the Projected Impact of Climate Change

The main objective of this study was to assess whether the widespread implementation of BGI practices could effectively adapt the actual UDS to the impact of climate change, particularly during an extreme rainfall event in the Pointe-aux-Trembles sector. The results presented in Figs. 4 and 5 indicate that the large-scale implementation of a combination of BGI practices, i.e., bioretention cells, permeable pavement, and green or blue roofs, successfully mitigated the projected impact of climate change on the hydrological performance of the UDS. Additionally, the combined BGI implementation scenarios not only counteracted the impact of climate change but also improved the UDS performance compared with historical responses, represented by a CCO indicator larger than 100%. In terms of flood risks, which can be highly damaging to municipalities, the widespread implementation of the simulated practices almost entirely prevented the UDS from overflowing in the entire study area, despite the significant increase in flood volume caused by the SICC [Fig. 5(e)].

Furthermore, apart from the BGI practices evaluated in this study, other practices could be considered to further support the UDS in the Pointe-aux-Trembles sector. For example, rain barrels collecting rainfall from sloped roofs or infiltration trenches treating runoff from sidewalks have shown promising potential in previous studies (Zahmatkesh et al. 2015; Ahiablame and Shakya 2016; Ghodsi et al. 2020). It becomes evident that at a district scale, the collective impact of implementing such small-scale practices can be significant. By rethinking the approach to managing rainfall in urban areas, societies have the potential to initiate city adaptation to climate change while also enhancing existing infrastructure performance. BGI practices can thus be considered as no-regret strategies (Hallegatte 2009) and should play a crucial role in climate change adaptation strategies.

Given the established potential of BGI practices to effectively adapt the current UDS to the impact of climate change, it becomes imperative to incorporate economic considerations into the evaluation of the feasibility of these solutions. Future research could involve a comparison of the implementation and maintenance costs associated with BGI practices, juxtaposed with an economic assessment of the multifaceted advantages they offer. These benefits might encompass the reduction in flood-related damages, financial savings derived from obviating the need for upgrading or constructing conventional gray infrastructure, mitigation of CSOs, and reducing the volume of runoff requiring treatment at wastewater treatment facilities.

Performance of BGI According to the Impervious Area Occupied

The percentage of impervious area occupied by BGI practices is a key factor influencing their effectiveness in mitigating the SICC on the response of the UDS (Table 3 and Figs. 3–5). Similar findings have been reported in previous studies (Palla and Gnecco 2015; Samouei and Özger 2020). However, some exceptions have been identified. For instance, in Subarea A, the BIO scenario exhibited lower modeling performance in mitigating flood volume despite having a higher implementation ratio of bioretention cells compared with the other subareas. Additionally, the BR scenario demonstrated lower modeling effectiveness in mitigating flood volume in Subarea B compared with Subareas A and C, despite having a similar BGI implementation ratio. These exceptions indicate

further factors beyond the implementation ratio may influence the effectiveness of BGI practices in specific subareas. Additional investigations are needed to fully understand these factors and improve the overall effectiveness of BGI implementation in urban areas.

Among the analyzed individual BGI scenarios, the BIO scenario demonstrated the highest potential in mitigating the impact of the SICC across all three metrics, despite having a smaller implementation ratio of bioretention cells compared with other BGIs (Table 3). This can be attributed to the fact that bioretention cells manage not only direct rainfall but also runoff from adjacent areas, resulting in the management of an impervious area that can be 10 times larger than their physical footprint. A study by Ahiablame and Shakya (2016) similarly found that BGI practices targeting runoff from roads were more effective in reducing flooding compared with practices focusing parking lots and rooftops because roads constitute a larger proportion of impervious surfaces. This suggests that bioretention cells, when widely implemented in urban areas, hold significant potential in mitigating the impacts of climate change on UDS performance while occupying a relatively small proportion of the total impervious area.

Influence of the Soil Conductivity Parameter on Green Roof Performance

The results emphasized the performance disparity between green roofs and blue roofs in mitigating the effects of the SICC on the response of the actual UDS during the design storm event (Figs. 3–5). As mentioned previously, this difference arises because the infiltration capacity of green roofs is exceeded by the intensity of rainfall, resulting in overflow into the network during the event. This renders green roofs less effective than blue roofs in mitigating peak flow from flat roofs and overall flood volume.

It is widely acknowledged in the literature that the performance of green roofs, particularly in terms of peak runoff, is sensitive to the soil conductivity parameter (Peng and Stovin 2017; Hamouz and Muthanna 2019; Liu and Chui 2019). In this study, the value of this parameter was chosen based on the work of Hamouz and Muthanna (2019), who determined a calibrated soil conductivity value of 11.1 mm/h for green roofs in cold climates using data from a full-scale experimental green roof. This value is also consistent with the calibrated value of 15 mm/h reported by Liu and Chui (2019), based on data from an experimental green roof, and falls within the range of the calibrated value of 38 mm/h found by Krebs et al. (2016). However, other studies have found significantly higher values for this parameter [e.g., calibrated values of 1,000 mm/h based on laboratory test measurements by Palla and Gnecco (2015) and Peng and Stovin (2017), and calibrated values ranging from 42 to 1,276 mm/h depending on the green roof type by Johannessen et al. (2019)]. Moreover, in practical applications, green roofs should be designed to prevent surface runoff (Peng and Stovin 2017; Liu and Chui 2019; Hamouz and Muthanna 2019). Therefore, the performance of green roofs simulated in this study may be conservative.

In order to assess the sensitivity of the soil conductivity parameter in the context of this study, a simulation was performed using a soil conductivity value of 100 mm/h. The results, represented in Fig. 6, demonstrated that the green roof scenario outperformed the blue roof scenario in mitigating both peak flow and flood volume under the same design storm event. This suggests that optimizing the infiltration capacity of the soil in green roofs to prevent overflow during extreme rainfall events could significantly enhance their potential to adapt the actual UDS to the impacts of climate change when implemented on a larger scale in urban areas.

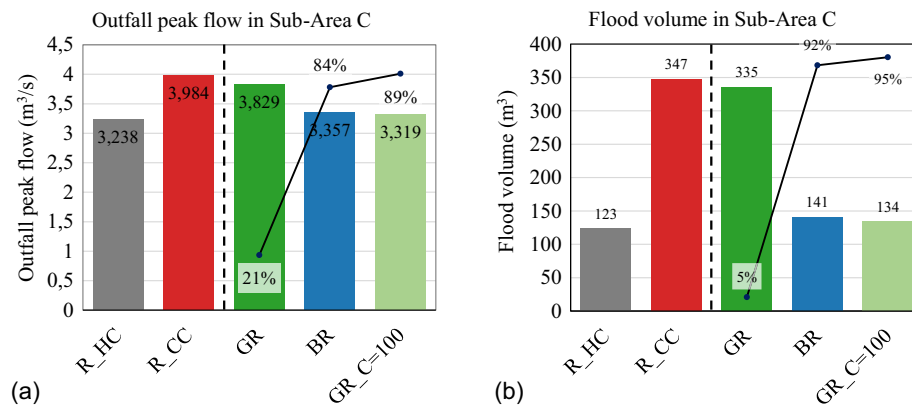


Fig. 6. Bar graphs of (a) outfall peak flow in Subarea C; and (b) flood volume in Subarea C for four simulated scenarios (R_HC, R_CC, GR, and BR) and for the green roofs scenario with a soil conductivity value of 100 mm/h instead of 12.5 mm/h (GR_C = 100) and CCO indicator values (solid curve) for runoff volume in the three BGI implementation scenarios.

Incertitude Regarding the Impact of Climate Change on Extreme Rainfall Events

Considering the significant uncertainty surrounding the impact of climate change on the intensification of extreme rainfall events, it is important to acknowledge that the recommended 18% increase in rainfall intensity may potentially be underestimated. Several studies have suggested the likelihood of higher increases for short-duration extreme rainfall events (Fowler et al. 2021; Martel et al. 2021). Therefore, conducting further research that incorporates hypotheses of stronger increases in rainfall intensity and explores other types of rainfall events would be valuable. This would contribute to a more comprehensive understanding of the potential impacts of climate change on urban areas.

In light of these future uncertainties, it is important to note that various BGI practices, including those evaluated in this study, offer the advantage of being more adaptable to future changes compared with traditional UDS. This adaptability stems from their surface location, which allows for easier modification or updating to accommodate evolving climate conditions (Samouei and Özger 2020). This flexibility is crucial in the face of changing climatic patterns and highlights the potential of BGI practices as adaptive solutions for urban stormwater management in the context of climate change.

Conclusion

This study aimed to assess the maximum potential of implementing four BGI practices, both individually and in combination, on a large scale to mitigate the anticipated effects of climate change on the UDS. Using a high-resolution 20- km^2 PCSWMM model of an urban catchment, the study focused on an event with a 3-h duration and 10-year return period.

The evaluated large-scale implementation scenarios of BGI practices, including green roofs or blue roofs on flat roofs, permeable pavement in parking lots, commercial and industrial areas, and bioretention cells for road runoff, effectively mitigated the projected impact of climate change on the UDS in relation to the selected design rainfall event. The simulated impact of an 18% increase in rainfall intensity, representing the effects of climate change, resulted in a 32% increase in runoff volume in the study area. However, the individual implementation scenarios of BGI practices offset between 15% and 45% of this increase, whereas the combination scenarios achieved offsets of 99% and 81%.

In terms of outfall peak flow, the simulated impact of climate change led to a 20% increase in the study area. However, the individual implementation scenarios offset between 5% and 142% of this increase, and the combination scenarios achieved offsets of 202% and 256%. Similarly, for flood volume, the simulated impact of climate change showed a 136% increase in the study area, indicating the vulnerability of the UDS to increased rainfall intensity. Nevertheless, the individual implementation scenarios offset between 20% and 118% of this increase, and the combination scenarios achieved offsets of 162% and 167%.

The implementation of BGI practices not only mitigated the effects of climate change but also enhanced the overall performance of the UDS compared with its historical response. This highlights the significant potential of widespread BGI practice implementation as a means of adapting the UDS to climate change. Further research could investigate the impact of such implementation under various rainfall extreme events and take into account economic constraints. Despite its limitations, this study offers valuable insights to city planners concerning the potential for a paradigm shift in stormwater management through the adoption of BGI practices for efficient runoff management.

Data Availability Statement

The results of the PCSWMM simulations leading to the conclusions of this study are available from the corresponding author upon reasonable request. The PCSWMM model used during the study is proprietary and confidential in nature and cannot be provided.

Acknowledgments

This study was funded by the Natural Sciences and Engineering Research Council of Canada (NSERC) through Jean-Luc Martel's Discovery Grant.

References

- Ahiablame, L., and R. Shakya. 2016. "Modeling flood reduction effects of low impact development at a watershed scale." *J. Environ. Manage.* 171 (Apr): 81–91. <https://doi.org/10.1016/j.jenvman.2016.01.036>.

- Akter, T., P. Quevauviller, S. J. Eisenreich, and G. Vaes. 2018. "Impacts of climate and land use changes on flood risk management for the Schijn River, Belgium." *Environ. Sci. Policy* 89 (Nov): 163–175. <https://doi.org/10.1016/j.envsci.2018.07.002>.
- Almaaitah, T., M. Appleby, H. Rosenblat, J. Drake, and D. Joksimovic. 2021. "The potential of blue-green infrastructure as a climate change adaptation strategy: A systematic literature review." *Blue-Green Syst.* 3 (1): 223–248. <https://doi.org/10.2166/bgs.2021.016>.
- Arisz, H., and B. C. Burrell. 2006. "Urban drainage infrastructure planning and design considering climate change." In *Proc., 2006 IEEE EIC Climate Change Conf.*, 1–9. New York: IEEE. <https://doi.org/10.1109/EICCCC.2006.277251>.
- CHI (Computational Hydraulics Inc.). 2023. "SWMM5 modeling with PCSWMM." Accessed November 17, 2023. <https://www.pcswmm.com/>.
- CSA (Canadian Standards Association) Group. 2018. *Design of bioretention systems*. CSA W200. Toronto: CSA Group.
- Ding, B., F. Rezaeehad, B. Gharedaghloo, P. Van Cappellen, and E. Passeport. 2019. "Bioretention cells under cold climate conditions: Effects of freezing and thawing on water infiltration, soil structure, and nutrient removal." *Sci. Total Environ.* 649 (Feb): 749–759. <https://doi.org/10.1016/j.scitotenv.2018.08.366>.
- Dong, X., H. Guo, and S. Zeng. 2017. "Enhancing future resilience in urban drainage system: Green versus grey infrastructure." *Water Res.* 124 (Nov): 280–289. <https://doi.org/10.1016/j.watres.2017.07.038>.
- Drake, J., A. Bradford, and T. Van Seters. 2014. "Hydrologic performance of three partial-infiltration permeable pavements in a cold climate over low permeability soil." *J. Hydrol. Eng.* 19 (9): 04014016. [https://doi.org/10.1061/\(ASCE\)HE.1943-5584.0000943](https://doi.org/10.1061/(ASCE)HE.1943-5584.0000943).
- Fletcher, T. D., et al. 2015. "SUDS, LID, BMPs, WSUD and more—The evolution and application of terminology surrounding urban drainage." *Urban Water J.* 12 (7): 525–542. <https://doi.org/10.1080/1573062X.2014.916314>.
- Fowler, H. J., et al. 2021. "Anthropogenic intensification of short-duration rainfall extremes." *Nat. Rev. Earth Environ.* 2 (2): 107–122. <https://doi.org/10.1038/s43017-020-00128-6>.
- Ghods, S. H., Z. Zahmatkesh, E. Goharian, R. Kerachian, and Z. Zhu. 2020. "Optimal design of low impact development practices in response to climate change." *J. Hydrol.* 580 (Jan): 124266. <https://doi.org/10.1016/j.jhydrol.2019.124266>.
- Hallegatte, S. 2009. "Strategies to adapt to an uncertain climate change." *Global Environ. Change* 19 (2): 240–247. <https://doi.org/10.1016/j.gloenvcha.2008.12.003>.
- Hamouz, V., and T. M. Muthanna. 2019. "Hydrological modelling of green and grey roofs in cold climate with the SWMM model." *J. Environ. Manage.* 249 (Nov): 109350. <https://doi.org/10.1016/j.jenvman.2019.109350>.
- Imran, H. M., S. Akib, and M. R. Karim. 2013. "Permeable pavement and stormwater management systems: A review." *Environ. Technol.* 34 (18): 2649–2656. <https://doi.org/10.1080/09593330.2013.782573>.
- IPCC (Intergovernmental Panel on Climate Change). 2021. *Climate change 2021: The physical science basis. Contribution of working group I to the sixth assessment report of the intergovernmental panel on climate change*, edited by V. Masson-Delmotte, et al. Cambridge, UK: Cambridge University Press. <https://doi.org/10.1017/9781009157896>.
- Johannessen, B. G., V. Hamouz, A. S. Gragne, and T. M. Muthanna. 2019. "The transferability of SWMM model parameters between green roofs with similar build-up." *J. Hydrol.* 569 (Feb): 816–828. <https://doi.org/10.1016/j.jhydrol.2019.01.004>.
- Johannessen, B. G., H. M. Hanslin, and T. M. Muthanna. 2017. "Green roof performance potential in cold and wet regions." *Ecol. Eng.* 106 (Sep): 436–447. <https://doi.org/10.1016/j.ecoleng.2017.06.011>.
- Krebs, G., K. Kuoppamäki, T. Kokkonen, and H. Koivusalo. 2016. "Simulation of green roof test bed runoff." *Hydrol. Processes* 30 (2): 250–262. <https://doi.org/10.1002/hyp.10605>.
- Lee, J. G., and J. P. Heaney. 2003. "Estimation of urban imperviousness and its impacts on storm water systems." *J. Water Resour. Plann. Manage.* 129 (5): 419–426. [https://doi.org/10.1061/\(ASCE\)0733-9496\(2003\)129:5\(419\)](https://doi.org/10.1061/(ASCE)0733-9496(2003)129:5(419)).
- LégisQuébec. 2022. "Loi sur la qualité de l'environnement. Chapitre Q-2, r. 9.01-Code de conception d'un système de gestion des eaux pluviales admissible à une déclaration de conformité." Accessed November 17, 2023. <https://www.legisquebec.gouv.qc.ca/fr/document/rc/Q-2,%20r.%209.01#se:39>.
- Leopold, L. B. 1968. *Hydrology for urban land planning: A guidebook on the hydrologic effects of urban land use*. Reston, VA: USGS.
- Liu, L., O. Fryd, and S. Zhang. 2019. "Blue-green infrastructure for sustainable urban stormwater management—Lessons from six municipality-led pilot projects in Beijing and Copenhagen." *Water* 11 (10): 2024. <https://doi.org/10.3390/w11102024>.
- Liu, X., and T. F. M. Chui. 2019. "Evaluation of green roof performance in mitigating the impact of extreme storms." *Water* 11 (4): 815. <https://doi.org/10.3390/w11040815>.
- Lotus Water. 2018. *Green infrastructure modeling and monitoring study—Technical memorandum: Evaluation and recommendations for green infrastructure modeling standards*. San Francisco: Lotus Water.
- Lotus Water. 2021. *Green infrastructure modeling study—Phase II: Evaluation and recommendations for green infrastructure modeling standards*. San Francisco: Lotus Water.
- Mailhot, A., and S. Duchesne. 2010. "Design criteria of urban drainage infrastructures under climate change." *J. Water Resour. Plann. Manage.* 136 (2): 201–208. [https://doi.org/10.1061/\(ASCE\)WR.1943-5452.0000023](https://doi.org/10.1061/(ASCE)WR.1943-5452.0000023).
- Mamo, T. G. 2015. "Evaluation of the potential impact of rainfall intensity variation due to climate change on existing drainage infrastructure." *J. Irrig. Drain. Eng.* 141 (10): 05015002. [https://doi.org/10.1061/\(ASCE\)IR.1943-4774.0000887](https://doi.org/10.1061/(ASCE)IR.1943-4774.0000887).
- Martel, J.-L., F. P. Brisette, P. Lucas-Picher, M. Troin, and R. Arsenault. 2021. "Climate change and rainfall intensity–duration–frequency curves: Overview of science and guidelines for adaptation." *J. Hydrol. Eng.* 26 (10): 03121001. [https://doi.org/10.1061/\(ASCE\)HE.1943-5584.0002122](https://doi.org/10.1061/(ASCE)HE.1943-5584.0002122).
- Martel, J.-L., A. Mailhot, and F. Brisette. 2020. "Global and regional projected changes in 100-yr subdaily, daily, and multiday precipitation extremes estimated from three large ensembles of climate simulations." *J. Clim.* 33 (3): 1089–1103. <https://doi.org/10.1175/JCLI-D-18-0764.1>.
- MDDEFP (Ministère du Développement durable, de l'Environnement, de la Faune et des Parcs). 2011. *Guide de gestion des eaux pluviales*. Québec: MDDEFP.
- Moriassi, D. N., J. G. Arnold, M. W. Van Liew, R. L. Bingner, R. D. Harmel, and T. L. Veith. 2007. "Model evaluation guidelines for systematic quantification of accuracy in watershed simulations." *Trans. ASABE* 50 (3): 885–900. <https://doi.org/10.13031/2013.23153>.
- Nazarnia, N., C. Schwick, and J. A. G. Jaeger. 2016. "Accelerated urban sprawl in Montreal, Quebec City, and Zurich: Investigating the differences using time series 1951–2011." *Ecol. Indic.* 60 (Jan): 1229–1251. <https://doi.org/10.1016/j.ecolind.2015.09.020>.
- Palla, A., and I. Gnecco. 2015. "Hydrologic modeling of low impact development systems at the urban catchment scale." *J. Hydrol.* 528 (Sep): 361–368. <https://doi.org/10.1016/j.jhydrol.2015.06.050>.
- Peng, Z., and V. Stovin. 2017. "Independent validation of the SWMM green roof module." *J. Hydrol. Eng.* 22 (9): 04017037. [https://doi.org/10.1061/\(ASCE\)HE.1943-5584.0001558](https://doi.org/10.1061/(ASCE)HE.1943-5584.0001558).
- Pour, S. H., A. K. Abd Wahab, S. Shahid, M. Asaduzzaman, and A. Dewan. 2020. "Low impact development techniques to mitigate the impacts of climate-change-induced urban floods: Current trends, issues and challenges." *Sustainable Cities Soc.* 62 (Nov): 102373. <https://doi.org/10.1016/j.scs.2020.102373>.
- Qin, H.-P., Z.-X. Li, and G. Fu. 2013. "The effects of low impact development on urban flooding under different rainfall characteristics." *J. Environ. Manage.* 129 (Nov): 577–585. <https://doi.org/10.1016/j.jenvman.2013.08.026>.
- Rossmann, L. A. 2015. *Storm water management model user's manual version 5.1*. Cincinnati: EPA.
- Rossmann, L. A. 2016. *Storm water management model reference manual. Volume III—Water quality*. Cincinnati: EPA.
- Samouei, S., and M. Özger. 2020. "Evaluating the performance of low impact development practices in urban runoff mitigation through

- distributed and combined implementation.” *J. Hydroinf.* 22 (6): 1506–1520. <https://doi.org/10.2166/hydro.2020.054>.
- Shafique, M., D. Lee, and R. Kim. 2016. “A field study to evaluate runoff quantity from blue roof and green blue roof in an urban area.” *Int. J. Control Autom.* 9 (8): 59–68. <https://doi.org/10.14257/ijca.2016.9.8.07>.
- Shamsi, U. M. S., and J. Koran. 2017. “Continuous calibration.” *J. Water Manage. Model.* 25: C414. <https://doi.org/10.14796/JWMM.C414>.
- Sohn, W., J.-H. Kim, M.-H. Li, and R. Brown. 2019. “The influence of climate on the effectiveness of low impact development: A systematic review.” *J. Environ. Manage.* 236 (Apr): 365–379. <https://doi.org/10.1016/j.jenvman.2018.11.041>.
- Statistics Canada. 2023. “Census profile. 2021 census of population. Statistics Canada Catalogue no. 98-316-X2021001.” Accessed May 17, 2023. <https://www12.statcan.gc.ca/census-recensement/2021/dp-pd/prof/index.cfm?Lang=F>.
- STEP (Sustainable Technologies Evaluation Program). 2022. “LID SWM planning and design guide.” *Sustainable Technologies Evaluation Program*. Accessed June 27, 2023. https://wiki.sustainabletechnologies.ca/index.php?title=Main_Page&oldid=15038.
- Suleiman, L. 2021. “Blue green infrastructure, from niche to mainstream: Challenges and opportunities for planning in Stockholm.” *Technol. Forecasting Social Change* 166 (May): 120528. <https://doi.org/10.1016/j.techfore.2020.120528>.
- Tansar, H., H.-F. Duan, and O. Mark. 2022. “Catchment-scale and local-scale based evaluation of LID effectiveness on urban drainage system performance.” *Water Resour. Manage.* 36 (2): 507–526. <https://doi.org/10.1007/s11269-021-03036-6>.
- USEPA. 2019. “Green infrastructure.” *Collections and Lists*. Accessed November 17, 2023. <https://www.epa.gov/green-infrastructure>.
- Versini, P.-A., N. Kotelnikova, A. Poulhes, I. Tchiguirinskaia, D. Schertzer, and F. Leurent. 2018. “A distributed modelling approach to assess the use of blue and green infrastructures to fulfil stormwater management requirements.” *Landscape Urban Plann.* 173 (May): 60–63. <https://doi.org/10.1016/j.landurbplan.2018.02.001>.
- Yang, Y., L. Sun, R. Li, J. Yin, and D. Yu. 2020. “Linking a storm water management model to a novel two-dimensional model for urban pluvial flood modeling.” *Int. J. Disaster Risk Sci.* 11 (4): 508–518. <https://doi.org/10.1007/s13753-020-00278-7>.
- Yu, M. M., J. W. Zhu, W. F. Gao, D. P. Xu, and M. Zhao. 2017. “Urban permeable pavement system design based on ‘sponge city’ concept.” *IOP Conf. Ser.: Earth Environ. Sci.* 82 (1): 012027. <https://doi.org/10.1088/1755-1315/82/1/012027>.
- Zahmatkesh, Z., S. J. Burian, M. Karamouz, H. Tavakol-Davani, and E. Goharian. 2015. “Low-impact development practices to mitigate climate change effects on urban stormwater runoff: Case study of New York City.” *J. Irrig. Drain. Eng.* 141 (1): 04014043. [https://doi.org/10.1061/\(ASCE\)IR.1943-4774.0000770](https://doi.org/10.1061/(ASCE)IR.1943-4774.0000770).